Check for updates

View Article Online
View Journal

JAAS

Accepted Manuscript

This article can be cited before page numbers have been issued, to do this please use: N. L. A. Jamari, J. F. Dohmann, A. Raab, E. Krupp and J. Feldmann, *J. Anal. At. Spectrom.*, 2017, DOI: 10.1039/C7JA00051K.

This is an Accepted Manuscript, which has been through the Royal Society of Chemistry peer review process and has been accepted for publication.

Accepted Manuscripts are published online shortly after acceptance, before technical editing, formatting and proof reading. Using this free service, authors can make their results available to the community, in citable form, before we publish the edited article. We will replace this Accepted Manuscript with the edited and formatted Advance Article as soon as it is available.

You can find more information about Accepted Manuscripts in the author guidelines.

Please note that technical editing may introduce minor changes to the text and/or graphics, which may alter content. The journal's standard Terms & Conditions and the ethical guidelines, outlined in our author and reviewer resource centre, still apply. In no event shall the Royal Society of Chemistry be held responsible for any errors or omissions in this Accepted Manuscript or any consequences arising from the use of any information it contains.

ROYAL SOCIETY OF CHEMISTRY

rsc.li/jaas

View Article Online
DOI: 10.1039/C7JA00051K

Journal Name

ARTICLE

NOVEL NON-TARGET ANALYSIS FOR FLUORINE COMPOUNDS USING ICPMS/MS AND HPLC-ICPMS/MS†

Received 00th January 20xx,
Accepted 00th January 20xx

DOI: 10.1039/x0xx00000x

www.rsc.org/

N. Laili A. Jamari,[a] J. Frederik Dohmann,[a] Andrea Raab,[a] Eva M. Krupp[a] and Joerg Feldmann*[a]

Measuring sub ppm levels of fluorine (F) directly with a commercial ICPMS is not possible due to high ionisation potential of F. Mixing of barium and fluorine solution enabled a new approach in fluorine analysis through the formation of the polyatomic ion BaF^+ using ICPMS/MS. Different parameters such as reaction gas flow rate, sampling position, nebuliser and make up gas flow rate, waiting and acquisition time as well as RF power were optimized in order to obtain the highest possible sensitivities for $^{138}Ba^{19}F^+$, as those parameters were important for polyatomic ions formation, avoiding barium oxide and barium hydroxide ions interference and sensitive detection in MS/MS. A limit of detection (LOD) of 0.043 mg L^{-1} was achieved with a good recovery of fluoride spiked in deionised water. For fluorine speciation analysis, coupling of anion exchange chromatography online to ICPMS/MS allowed separation and fluorine specific detection of fluoride and fluoroacetate. The response was compound independent as expected for ICPMS. The LOD for fluoride and fluoroacetate were 0.022 mg L^{-1} and 0.11 mg L^{-1} respectively. Both compounds were baseline separated and detected quantitatively, making this newly developed method a promising candidate for non-target fluorine speciation analysis in environmental samples.

Introduction

Fluorine plays an important role in human nutrition, as the daily intake of fluoride (F^-) can improve dental health through its cariostatic properties.[1,2] In some countries, a sufficient supply of the population with F^- is ensured by the fluoridation of drinking water.[3] Contrary to this, high concentrations of F^- in drinking water can lead to chronic toxic effects such as dental or skeletal fluorosis.[4–7] Analytical tools such as ion chromatography (IC) and ion-selective electrode measurements (ISE) are commonly used to monitor fluoride levels in water samples.[7–9] However, conventional IC is not specific to the detection of fluoride, as the separation is only based on the ionic strengths of the analytes and unspecific conductivity detection. Thus, co-elution with other compounds can lead to an overestimation of fluoride contents.[10] ISE methods are limited by matrix effects[8] from ions such as Si^{4+}, Fe^{3+} or Al^{3+}, which complex F^- ions and thereby lower the detected concentrations.

Besides fluoride, fluorinated organic compounds are released into the environment in large quantities from anthropogenic sources. Poly- and perfluorinated surfactants, such as perfluorooctanoic acid (PFOA), perfluorooctane-sulfonamide (PFOSA) or perfluorooctanesulfonic acid (PFOS) have been produced in exceed for industrial purposes and can be found in a variety of environmental samples.[11] Other compounds of interest are short-chained fluorinated acids such as trifluoroacetic acid (TFA), which originates from the atmospheric degradation of refrigerants and anaesthetics or from decombustion of perfluorinated polymers.[12,13] Fluoroacetic acid (FAA) is a highly toxic compound which naturally occurs in certain plants,[14] can be a metabolite formed by bacteria but has also been anthropogenically used as a pesticide.[15,16] Analysis of those organofluorine compounds is carried out via targeted quantification methods, such as molecular mass spectrometry using isotopically labelled standards.[17,18]

Approximately 20% of today's pharmaceutical products contain organofluorines, resulting in a broad variety of partially unknown metabolites and degradation products.[19] Despite their potentially toxic effects on biota, the environmental fate of those compounds is not always known and requires monitoring.[20] Mass balance approaches support this view by indicating the existence of so far unidentified organofluorines in for example seawater.[21] Targeted analysis methods as mentioned above are applicable only for known analytes. Thus, a non-targeted fluorine-specific approach to the analysis of environmental samples could be used to identify, quantify and monitor formerly unknown organofluorines.

Other fields of analytical chemistry, such as the research on organoarsenic compounds, have seen immense developments after the introduction of non-targeted speciation methods based on liquid chromatography (LC)

[a] Trace Element Speciation Laboratory (TESLA), Department of Chemistry, University of Aberdeen, Aberdeen, AB24 3UE, United Kingdom. Email: j.feldman@abdn.ac.uk

† Electronic Supplementary Information (ESI) available. See DOI: 10.1039/x0xx00000x

This journal is © The Royal Society of Chemistry 20xx

Please do not adjust margins

Published on 06 April 2017. Downloaded by University of Aberdeen on 12/04/2017 12:08:14.

Journal of Analytical Atomic Spectrometry Accepted Manuscript

View Article Online
DOI: 10.1039/C7JA00051K

Published on 06 April 2017. Downloaded by University of Aberdeen on 12/04/2017 12:08:14.

coupled to element specific detection methods as inductively coupled plasma mass spectrometry (ICPMS) or inductively coupled plasma optical emission spectrometry (ICPOES).[22,23] However, no suitable speciation methods for fluorinated organic compounds exist so far, mainly caused by the lack of powerful fluorine specific detection methods. Major challenges for the development of such a method are the high ionisation potential (17.418 eV) of F and the location of its resonance line in the vacuum ultraviolet range (95 nm).[24,25]

Low ionisation yields for the formation of F^+ ions and high occurring background levels due to interferences, such as $^{16}O^1H_3^+$, $^{18}O^1H^+$ and $^{17}O^1H_2^+$ ions are limiting factors to the practicality of positive mode ICPMS.[26–28] Therefore, Vickers et al. investigated the analysis of fluorine and other halogens using negative ion mode ICPMS.[29] A comparably lower background could be observed, resulting in a LOD of 400 µg L^{-1} for fluorine. Despite their high potential for the analysis of halogens, ICPMS instruments capable of switching between positive and negative ion modes are not commercially available nowadays. High resolution ICPMS offers another way to decrease the background from interfering ions, however the LOD for fluorine detection was too high for realistic concentration in environmental and medical applications (5.1 mg L^{-1}).[28]

Several molecular high temperature continuous source molecular absorption spectrometry methods (CS-MAS) were used to detect F indirectly through measuring the absorption of diatomic molecules, such as CaF or GaF.[30,31] CS-MAS method using GaF as the target analyte was used as a detector for chromatography.[32,33] Qin et al. were able to detect with the HPLC-CS-MAS a new fluorometabolite in *Streptomyces* media and thereby demonstrated the advantages of fluorine specific detection methods.[33] However, CS-MAS does not allow online coupling with chromatographic separation methods and is therefore limited in its application. A new approach to fluorine specific analysis using ICPMS/MS has been suggested by Yamada.[34] Through the online addition of barium solution to fluorine containing samples, the formation of polyatomic BaF^+ ions was enabled. Due to ^{138}Ba being the most abundant isotope, highest sensitivities would be achieved for $^{138}Ba^{19}F^+$ (*m/z* 157). Potential polyatomic ions formation mechanisms are shown in equations 1 and 2.

$$^{138}Ba^+ + {}^{19}F^o \rightleftharpoons {}^{138}Ba^{19}F^+ \quad (1)$$

$$^{138}Ba^{2+} + {}^{19}F^- \rightarrow {}^{138}Ba^{19}F^+ \quad (2)$$

Even though this approach bypasses the issue of low ionisation yields for F, it would still be limited by potential interfering ions with the same mass-to-charge ratio (*m/z*), such as $^{138}Ba^{18}O^1H^+$, $^{138}Ba^{16}O^1H_3^+$, and $^{138}Ba^{17}O^2H^+$. The occurring interferences can be reduced through a collision/reaction cell between the first and the second mass analyser in the MS/MS mode. MS/MS was used in this study as it has more power in reducing the interferences compared to single quadrupole ICPMS. The first quadrupole in MS/MS act as a mass filter by eliminating all ions except the target mass ions (*m/z* 157). By only allowing *m/z* 157 pass through Q1, the interferences coming from different masses such as $^{141}Pr^+$ or $^{140}Ce^+$, which might form polyatomic ions with the m/z 157 ($^{141}Pr^{16}O^+$, $^{140}Ce^{16}O^1H^+$) were eliminated. The interfering ions such as $^{157}Gd^+$ or $^{138}Ba^{18}O^1H^+$ have the same mass as the target analyte could be eliminate using reaction gas in collision/reaction cell. This helps in improving the performance in collision/reaction cell as the reaction gas can react with interfering ions but not the target polyatomic ions. In this study, the utilisation of a fluorine polyatomic ion formation was investigated and its use for the development of an online speciation method with HPLC separation and fluorine specific detection was evaluated. As a proof of concept, anion exchange chromatography HPLC was coupled online to ICPMS/MS and fluoride and FAA was separated, detected and quantified.

Experimental section

Chemicals, standards and reagents

Deionised water (18 MΩ cm, Smart2Pure, Thermo Fisher Scientific, UK) has been used for all analytical purposes. Calibration and spiking solutions were prepared from potassium fluoride (Fisher Scientific, UK), while barium solutions were prepared from barium nitrate (BDH, UK). Stock solutions of fluoroacetate (FAA) were prepared from sodium fluoroacetate (Aldrich Chemical Company, UK) and buffer solutions were prepared from ammonium carbonate (Fisher Scientific, UK).

Instrumental setup

ICPMS/MS. Analysis and method development was carried out using a 8800 Triple Quadrupole ICPMS/MS instrument (Agilent Technologies, UK) with a Micromist nebuliser for sample introduction, a quartz torch, a sampler and skimmer cone made from nickel, and S-lens. In order to enable BaF^+ formation, barium solution (0.22 mL min^{-1}) was mixed online with F containing samples or standards (0.33 mL min^{-1}) via a T-pin at a mixing ratio of 1:1.5. The ICPMS/MS was tuned daily for maximum sensitivity using a solution containing Co, Y, Ce, Tl, and Ba (1 µg L^{-1} each). The study aimed to optimize for maximum $^{138}Ba^{19}F^+$ sensitivity on *m/z* 157. Table 1 lists the investigated parameters and the optimized values are summarized in Table 2.

Table 1 Investigated parameters for method development.

Parameter	Values
Reaction gas	No gas, oxygen, hydrogen, and oxygen/hydrogen mixture
Oxygen flow rate (reaction gas)	0.10, 0.30, 0.50, 0.75 and 1.0 mL min^{-1}
RF power	600 – 1600 W
Sampling position	6.0 – 25.0 mm
Nebulizer gas flow rate	0.70 – 1.30 L min^{-1}
Make up gas flow rate	0.10 – 0.60 L min^{-1}
Ba concentration	10, 15, 28, 50 and 100 mg L^{-1}
Acquisition time	0.1 – 1.5 s

This journal is © The Royal Society of Chemistry 20xx

Please do not adjust margins

Journal of Analytical Atomic Spectrometry Accepted Manuscript

View Article Online
DOI: 10.1039/C7JA00051K

Published on 06 April 2017. Downloaded by University of Aberdeen on 12/04/2017 12:08:14.

Wait time offset	0 – 50 ms

HPLC-ICPMS/MS. For chromatography, an Agilent 1290 HPLC system with a PRP-X100 Hamilton anion exchange column (4.1 mm x 250 mm) was used. Ammonium carbonate (30 mM, pH 8.7) was used as mobile phase at an isocratic flow rate of 1 mL min^{-1}. A 100 µL sample loop was used for sample introduction. For the coupling, a transfer capillary was connecting the chromatographic column to the nebulizer of the ICPMS/MS system via a T-pin, which allowed the introduction of Ba solution. As the flow rate of HPLC was higher than fluorine standards or samples used in ICPMS/MS, therefore a higher Ba concentration was used (45 mg L^{-1}, flow rate 0.22 mL min^{-1}) to maintain the Ba concentration after mixing at the same level as in ICPMS/MS.

Results and discussions

Method optimization

Reaction gas. The capability of the method to monitor the signal of $^{138}Ba^{19}F^+$ at *m/z* 157 free from interferences is an important requirement for F to be detected successfully. Different gas modes for the collision/reaction cell of the ICPMS/MS were investigated. A high F sensitivity and signal-to-background ratio (SBR) was observed for O_2 as reaction gas (Fig. 1, and ESI-1). A product ion scan of ions in blank and 1 mg L^{-1} F solution with *m/z* 157 in first quadrupole (Q_1) was carried out and the entire mass spectrum was scanned using the second quadrupole (Q_2). Product ions such as $^{16}O_2^+$ (*m/z* 32), $^{138}Ba^+$ (*m/z* 138), $^{138}Ba^{16}O^+$ (*m/z* 154), $^{138}Ba^{16}O^1H$ (*m/z* 155), and $^{138}Ba^{16}O_2^+$ (*m/z* 170) were detected in the MS/MS spectra from the mother ions of *m/z* 157 (Fig. 2). The intensities of these ions were independent of the introduced fluoride concentration (Fig. ESI-2). Hence, it is likely that they were the MS/MS product of the following ions on m/z 157: $^{138}Ba^{18}O^1H^+$, $^{138}Ba^{17}O^2H^+$ and $^{138}Ba^{16}O^1H_3^+$. The signal intensity at *m/z* 157 increase when F was introduced (Fig. 2B), which give an evidence about the efficiency of $^{138}Ba^{19}F^+$ ions formation process. The use of oxygen as a reaction gas for the elimination of interfering ions in MS/MS mode is illustrated schematically in Fig. ESI-3.

Table 2 Optimum instrument settings for the determination of the $^{138}Ba^{19}F^+$.

Plasma	
RF power	1500 W
Sampling position	8.0 mm
Nebuliser gas flow rate	1.00 L min^{-1}
Makeup gas flow rate	0.37 L min^{-1}
Lenses	
Extract 1	-150.0 V
Extract 2	5.0 V
Deflect	-48.0 V
Cell	
Oxygen flow rate	0.75 mL min^{-1}
OctP Bias	-60.0 V
OctP RF	200 V
Energy Discrimination	-10.0 V
Wait Time Offset	2 ms

Five different O_2 flow rates were evaluated by comparing the intensities for *m/z* 157 of a blank solution and F containing solution (1 mg L^{-1}). The highest SBR of BaF^+ and sensitivity were found for O_2 flow rate of 0.75 mL min^{-1} (Fig. 3). Thus, in further analysis, $^{138}Ba^{19}F^+$ was detected in MS/MS mode, both Q_1 and Q_2 set at *m/z* 157 with 0.75 mL min^{-1} O_2 as a reaction gas.

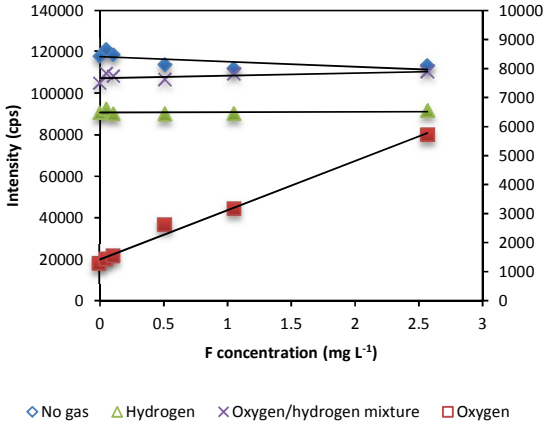

Fig. 1 The calibration graph of F in different gas modes; no gas, hydrogen, oxygen/hydrogen mixture displayed to the left Y-axis while the oxygen mode is displayed on the right Y-axis.

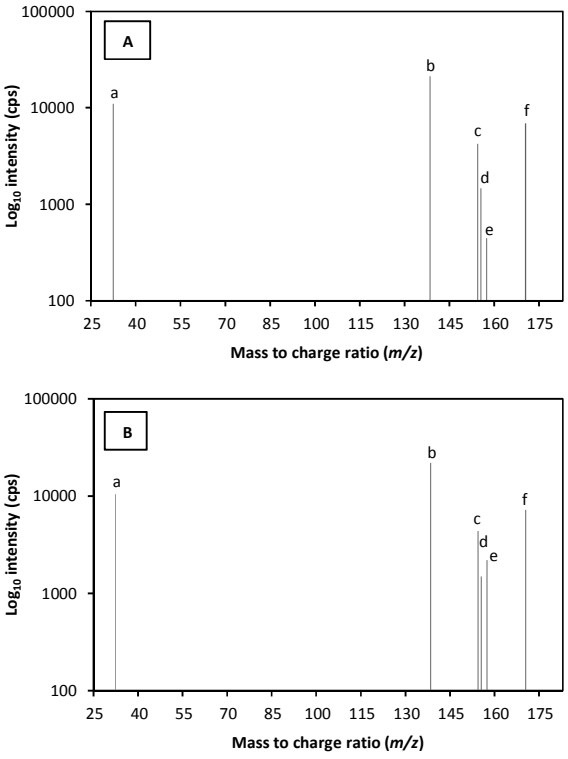

Fig. 2 MS/MS spectra: The reaction product ions scan of *m/z* 157 using oxygen as reaction gas in (A) blank and (B) 1 mg L^{-1} F solution

Journal of Analytical Atomic Spectrometry Accepted Manuscript

Please do not adjust margins

View Article Online
DOI: 10.1039/C7JA00051K

Published on 06 April 2017. Downloaded by University of Aberdeen on 12/04/2017 12:08:14.

mixed online with 15 mg L^{-1} Ba. (a) *m/z* 32 being $^{16}O_2^+$, (b) *m/z* 138 ($^{138}Ba^+$), (c) *m/z* 154 ($^{138}Ba^{16}O^+$), (d) *m/z* 155 ($^{138}Ba^{16}O^1H^+$), (e) *m/z* 157 ($^{138}Ba^{19}F^+$ and other barium interfering ions), and (f) *m/z* 170 ($^{138}Ba^{16}O^{16}O^+$).

Instrument settings and data acquisition parameters. Plasma conditions are crucial for the successful formation of $^{138}Ba^{19}F^+$ polyatomic ions. Hence, forward RF power was changed and subsequently optimised to gain maximum sensitivity by re-adjusting the sampling position and the gas flow rates. The first and the second quadrupole was set to a fixed *m/z* of 157 and the signal in blank and 1 mg L^{-1} fluoride containing solution was monitored. The signal intensities of the interfering ions and the efficiency of BaF^+ formation were changed with RF power. At low power, the signal is mainly produced by the interfering ions since the signal intensity of the blank is as high as the signal intensity for the fluoride solution, with increasing power the SBR of BaF^+ increases sharply. This would mean that the highest power should be used to gain highest sensitivity for $^{138}Ba^{19}F^+$ formation ions (see Fig. 4).

Sampling position was also independently optimised by measuring $^{138}Ba^{19}F^+$ intensities (*m/z* 157) for a solution containing F (5 mg L^{-1}) and subtracting the respective background intensities of a measured blank. The resulting values indicate a maximum intensity at approximately 7.8 mm sampling position (Fig. 5). Intensities of *m/z* 157 for blank and F containing solution are provided in Fig. ESI-4. For further analysis, a sampling position of 8.0 mm was used.

Nebuliser gas flow rates (0.7-1.3 L min^{-1}) and make up gas flow rates (0.1-0.6 L min^{-1}) were also optimised and the SBR of BaF^+ between F containing solution (5 mg L^{-1}) to blank was observed. The highest ratio was found to be around 0.94 L min^{-1} and 0.36 L min^{-1} of Ar flow rate for nebulizer and make up gas flow rate respectively. Both flow rates influence each other as the maximum SBR of BaF^+ of the total gas flow through the injector was found around 1.36 L min^{-1} (Fig. 6). The SBR of BaF^+ decreased when the flow increases. This indicates that the plasma cooling effect from the increased flow prevent the formation of sufficient BaF^+.

Intensities of Ba^+ and Ba^{2+} ions in dependence on the sampling position and total gas flow rates were monitored in search of possible correlations which Ba ions (Ba^+ or Ba^{2+}) play a role in $^{138}Ba^{19}F^+$ polyatomic ions formation. Such correlations could provide insight in regards to the polyatomic ions formation mechanism according to equation 1 and 2. For the determination of $^{132}Ba^{2+}$ signal intensities, a background of $^{66}Zn^+$ interferences had to be taken into account. The background intensities of $^{66}Zn^+$ were determined by measuring intensities of $^{70}Zn^+$ and calculating the intensity of $^{66}Zn^+$ based on isotopic abundances**.** The normalised intensity maxima of Ba^+ and Ba^{2+} were shifted to bigger sampling position and lower total gas flow rates compared to the maximum BaF^+ signal and SBR (Fig. 5 and Fig. 7). This indicates that both Ba^+ and Ba^{2+} were involved in the formation of BaF^+ depending on the type of F (either F^o and F^-) present in the plasma.

In order to see the effect of gas flow on polyatomic ions formation, BaO^+ ions was also monitored at *m/z* 148 for both Q_1 and Q_2. The maximum SBR of BaF^+ was found in between the maxima of Ba^+, Ba^{2+} and BaO^+ normalised intensities as a factor of total gas flow rates (Fig. 7). This indicates that the cooling effect, due to increased total gas flow rates up to a certain flow range, accelerates the formation of BaO^+. Since Ba are known as an easily oxidise element, while O atom are more abundant than Ba^+ ions and F in the plasma, BaO^+ tend to be produce. As

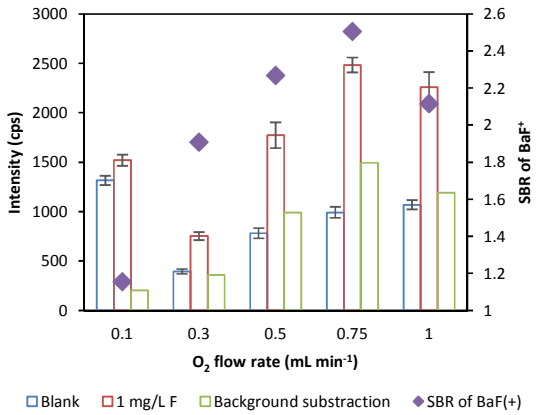

Fig. 3 SBR of BaF^+ (diamond) and intensity of *m/z* 157 counts for blank, 1 mg L^{-1} fluorine and background subtraction (bars) on different oxygen flow rates in reaction cell. Highest SBR for $^{138}Ba^{19}F^+$ is observed for a flow rate of 0.75 mL min^{-1}.

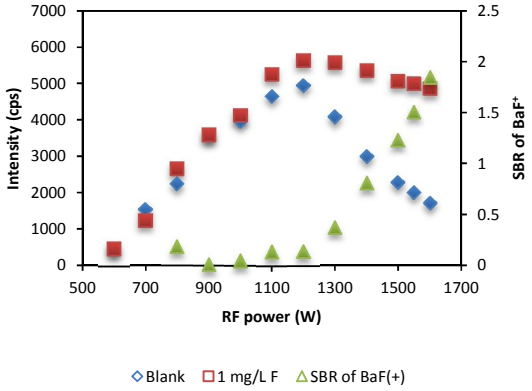

Fig. 4 The intensity at *m/z* 157 in blank and 1 mg L^{-1} F containing solution and SBR of $^{138}Ba^{19}F^+$ at different RF power. The intensity in blank (without F) and 1 mg L^{-1} F solution are displayed to the left Y-axis, while the SBR of BaF^+ is displayed on right Y-axis

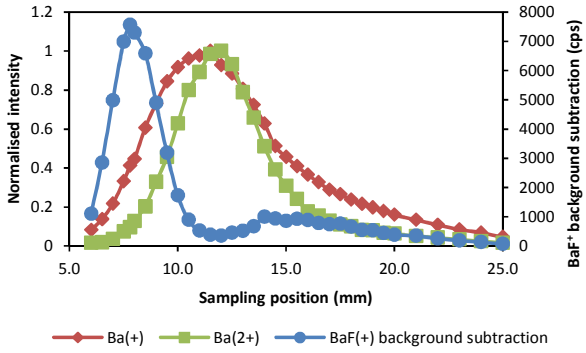

This journal is © The Royal Society of Chemistry 20xx

Please do not adjust margins

Journal of Analytical Atomic Spectrometry Accepted Manuscript

View Article Online
DOI: 10.1039/C7JA00051K

Published on 06 April 2017. Downloaded by University of Aberdeen on 12/04/2017 12:08:14.

Fig. 5 Background subtracted intensity for F containing solution (5 mg L^{-1}) and normalised intensities of Ba^+ and Ba^{2+} dependant on the sampling position. BaF^+signal illustrated on the right Y-axis, while normalised intensities of of Ba^+ and Ba^{2+} illustrated on left Y-axis.

the total gas flow rate decrease, the plasma becomes hotter, hence promotes the dissociation of BaO^+ into Ba^+ and O as shown in equation 3, which simultaneously begins the formation of BaF^+ from the reactants of Ba^+ and F^o. Further decrease in total gas flow promotes the dissociation of BaF^+ leading to the increase of Ba^+ ions. Thus, the formation of BaF^+ in equation 1 occurs in a certain range of the total gas flow rates. The BaF^+ formation through the reaction of equation (2) also occurs within certain range of total gas flow rate. As the total gas flow rates decreases, the plasma getting hotter. This cause the electron tends to leave the F^- anion and forming the neutral F^o. Hence, BaF^+ formation will be suppressed if the flow rate is too low. Apart from that, when the total gas flow rate increases, the plasma gets cooler causing the ionisation yield of Ba^{2+} decreases. Hence, BaF^+ formation will be suppressed if the flow rate is too high. This means that the lack of either one of the reactants, Ba^{2+} or F^- prevents the formation of BaF^+ through the reaction in equation (2).

$$Ba^+ + O \rightleftharpoons BaO^+ \qquad (3)$$

The sharp maximum of the background subtraction for BaF^+ detection in sampling position indicates that the optimum formation conditions for BaF^+ can only be found in a small part of the plasma, which is not ideal for getting a stable signal. This was also evident in the nebuliser flow variation. Variable plasma conditions through variation of the introduced samples or solvent flow could potentially result in large intensity variations, which would not be desirable. Not only the maximum SBR of BaF^+ was a sharp peak, it seems also that the plasma was sampled in the hottest zone and not as expected in the recombination zone. This also confirms the highest SBR of BaF^+ was recorded with the highest RF power used.

The concentration of the used Ba solutions was also optimised. Different Ba concentrations were mixed online with blank and 1 mg L^{-1} F containing solution at a fixed mixing ratio of 1:1.5. The results shown in Fig. 8 indicate that by increasing Ba concentration, the counts for *m/z* 157 and the standard deviation (SD) of 10 measurements increases. Thus, as a compromise between the small SD and sufficient BaF^+ intensity, 15 mg L^{-1} of Ba was chosen for further analysis. The lower Ba concentration reduces also the risk of clogging the skimmer cone. The Ba concentration is however still high enough that ppb levels of barium in the sample would not significantly change the BaF^+ formation.

According to Resano *et al.* [35], a sufficiently high counts of ions is an indicator for the best performance of ICPMS through a combination of long acquisition time with fast scanning. Different acquisition times for *m/z* 157 intensities and wait time offsets (WTO) using 10 replicates for each measurement in blank and 1 mg L^{-1} F containing solution were evaluated. Acquisition times in the range of 0.1 s to 1.0 s were tested and the result was shown in Fig. ESI-5. As the acquisition time increase, the SD illustrated as error bar was improved. Thus, an acquisition time of 1.0 s for each replicate measurement was chosen for further analysis. WTO allows the MS/MS system to reach a steady state for the detection of ions when using a collision/reaction cell.[36] However, changes to the WTO showed no significant effects towards the measured intensities for $^{138}Ba^{19}F^+$ (Fig. ESI-6). For future measurements, a WTO of 2 ms was used.

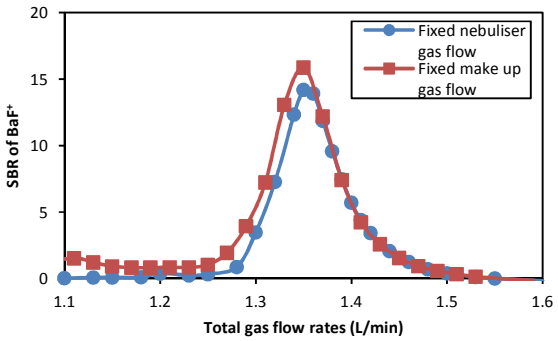

Fig. 6 SBR of $^{138}Ba^{19}F^+$ of total gas flow rates between 5 mg L^{-1} F containing solution to blank. The highest SBR was found around 1.36 L min^{-1} of total gas flow rate for both nebuliser and make up gas flow.

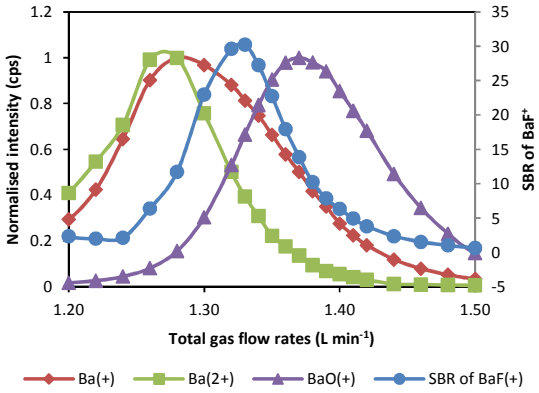

Fig. 7 Normalised intensity of Ba^+, Ba^{2+} and BaO^+, and SBR of BaF^+ as a function to total gas flow rates in blank and 5 mg L^{-1} F containing solution. The normalised intensity of Ba^+, Ba^{2+} and BaO^+ displayed on the left Y-axis, while SBR of BaF^+ displayed on right Y-axis.

Journal of Analytical Atomic Spectrometry Accepted Manuscript

Please do not adjust margins

View Article Online
DOI: 10.1039/C7JA00051K

Published on 06 April 2017. Downloaded by University of Aberdeen on 12/04/2017 12:08:14.

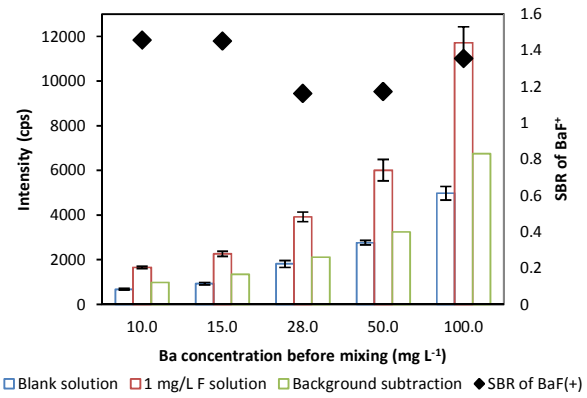

Fig. 8 SBR of BaF^+ (diamond) and intensity of *m/z* 157 counts in the presence of F, without F and background subtraction (bars) on different Ba concentrations; 10, 15, 28, 50 and 100 mg L^{-1}. The background and SD increase as Ba concentration increases. Small SD and sufficient BaF^+ signal are observed for 15 mg L^{-1} Ba.

The presence of $^{157}Gd^+$ in the sample might interfere with the detection and quantification of $^{138}Ba^{19}F^+$ as they have the same mass (*m/z* 157). Therefore, the interference of concomitant Gd was studied. Under the optimised conditions for BaF^+ would allow $^{157}Gd^+$ through Q_1, but only 8% of the Gd^+ appeared on *m/z* 157, while the rest was oxidised in the collision/reaction cell by oxygen to GdO^+ with a mass shift to *m/z* 173 (Fig. ESI-7). Nevertheless, approximately 100 µg L^{-1} Gd would simulate 500 µg L^{-1} F. Hence, in the presence of possible Gd in the sample, it would be recommended to optimise the reaction gas flow for a more efficient oxidation of Gd.

Figure of merits and determination of fluorine

Total F concentration by ICPMS/MS. By allowing *m/z* 157 in MS/MS mode, a linear equation of y = 3229.1 x + 1881.7 and R^2= 0.991 was obtained with a 6 points calibration. The LOD and limit of quantification (LOQ) of F were calculated from 3 SD and 10 SD of the blank value and were found to be 0.043 mg L^{-1} and 0.086 mg L^{-1} respectively (calculations see ESI).

The capability of the developed method was evaluated by spiking approximately 1 mg L^{-1} fluoride standard into water. The measurement was done in triplicates with 10 replicates in each measurement and the result shows the F concentration of 0.95 ± 0.058 mg L^{-1} with a recovery of 97 ± 4%. From *t*-test analysis, with 95% confidence interval (CI), the result of p-value ≥ 0.05 indicating the expected and the measured F concentration has similar concentration (Table ESI-1). Additionally, the data on triplicate measurements and 10 replicates in each measurement showed acceptable reproducibility with 2.4-5.8% RSD (Table ESI-2). The relative high RSD may be explained by the sharp maximum in the plasma when optimised the sampling position and total gas flow rates. But overall the achieved performance suggests that the method is sensitive and reliable for at least fluoride analysis and can potentially be used for total fluorine environmental analysis.

One condition for total fluorine analysis would be to test whether the sensitivity of fluorine as BaF^+ is independent of the fluorine containing species or not. Since this study focussed on a speciation study, the species-specific sensitivity was tested using the online HPLC coupled to ICPMS/MS.

Speciation by HPLC-ICPMS/MS. For speciation analysis of different F compounds, HPLC was coupled to ICPMS/MS method. Two F compounds (fluoride and fluoroacetate) were mixed to the same concentration with regards to the F-content. Both compounds were baseline separated within 15 minutes through isocratic elution of 30 mM ammonium carbonate (Fig. 9). The chromatogram showed that fluoride has a sharper peak compared to fluoroacetate peak; however, both compounds have similar sensitivities with regard to their F content indicating compound independent fluorine specific detection (Fig. 10). Similar results were obtained for HR-ICPMS analysis of fluorinated compounds,[28] proving that the argon plasma of ICPMS is powerful enough to cleave even the strongest of single bonds in organic compounds, ie. C-F bond, without a shift in the BaF^+ formation. This indicates that not only fluoride but also other fluorine containing compounds can be quantified using fluoride as a standard. This would be useful for the determination of total fluorine in a sample containing multiple organofluorine species and for quantifying unknown F containing compounds with regards to their F content.

The LOD of HPLC-ICPMS/MS method for individual species was comparable to that for fluorine without chromatography. The calibration data, instrumental LOD and LOQ of each compound are listed in Table 3. Both LOD and LOQ were calculated based on 3 SD and 10 SD of the blank value and were found to be 0.022 mg L^{-1} and 0.085 mg L^{-1} for fluoride, while 0.11 mg L^{-1} and 0.18 mg L^{-1} for fluoroacetate (calculation see ESI). The absolute LOD for fluoride was 2.2 ng; while for fluoroacetate is 11 ng F as fluoroacetate. Increasing the sample loop to 1.000 mL would potentially decrease the LOD to single figure µg L^{-1} concentrations if chromatographic separation is not the first priority. In comparison with the published methods, the newly developed method is not only able to detect fluorine specifically but also has a comparably low LOD (Table 4).

Three water samples containing approximately 1 mg L^{-1} of F for each compound were analyse. The HPLC-ICPMS/MS measurements were carried out with triplicate injections. Based on the results (Table 5), the concentration of F in fluoride and fluoroacetate in a good agreement with recoveries of 91% ± 6% to 96 % ± 11% respectively. Via *t*-test analysis, with 95% CI, the concentration spiked and the concentration measured by the speciation method have similar mean concentrations for both compounds (p-values ≥ 0.05) (Table ESI-3). This suggests that the method is F specific.

Furthermore, another advantage to use HPLC-ICPMS/MS for fluorine detection might be the potential of reducing interferences from metal ions in the samples, which might influence the BaF^+ or interfering ions formation detected on *m/z* 157. The metal such as Gd, Pr or additional Ba in the sample can be separated from the fluorine species by the used chromatography. Hence, the use of chromatography can potentially be used for matrix separation and enhance the robustness of the fluorine detection.

This journal is © The Royal Society of Chemistry 20xx

Journal of Analytical Atomic Spectrometry Accepted Manuscript

Please do not adjust margins

View Article Online
DOI: 10.1039/C7JA00051K

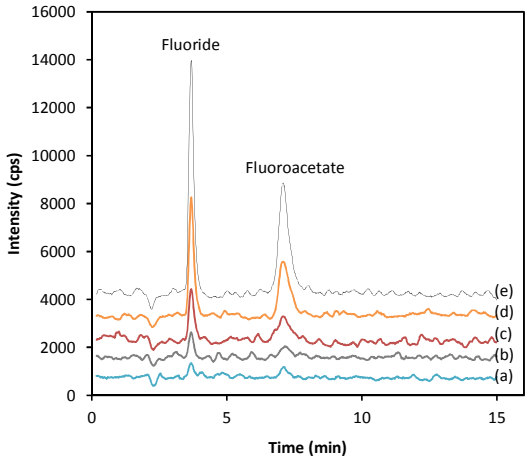

Fig. 9 The HPLC-ICPMS/MS chromatogram of fluoride and fluoroacetate in different F concentrations: (a) 0.25 mg L^{-1} (b) 0.5 mg L^{-1} (c) 1.0 mg L^{-1} (d) 2.5 mg L^{-1} (e) 5.0 mg L^{-1}. Both compounds were detected at *m/z* 157.

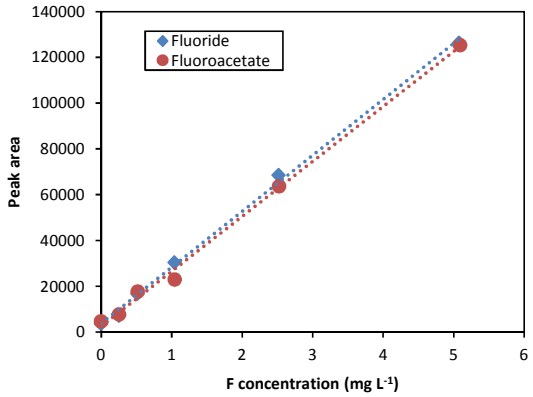

Fig. 10 The HPLC-ICPMS/MS calibration graph of fluorine compounds; fluoride and fluoroacetate.

Conclusions

In this work, the newly developed method for F analysis through the formation of $^{138}Ba^{19}F^{+}$ using ICPMS/MS was demonstrated. $^{138}Ba^{19}F^{+}$ was efficiently formed at 1500 W RF power and in the presence of 0.75 mL min^{-1} O_2 as a reaction gas, the interfering barium polyatomic ions were reduced. Although the mechanism how BaF^{+} is generated was not studied in detail, the high power, low total gas flow and small sampling position would indicate that both Ba^{+} and Ba^{2+} play important roles in BaF^{+} formation depending on the types of F, either atomic F^{o} or negative fluorine F^{-}. The developed method enables the total F determination by ICPMS/MS with good recovery, 0.043 mg L^{-1} LOD and acceptable reproducibility. Coupling of HPLC directly to ICPMS/MS enabled the first speciation method for non-target analysis of F-containing compounds analysing F species with 0.022 mg L^{-1} and 0.11 mg L^{-1} LOD for fluoride and FAA respectively. In conclusion, the developed method offers the first method for a simple and fast way for a sensitive, specific, and reliable F analysis at relevant levels and opens up new possibilities for the future analysis of environmental samples.

Acknowledgements

NLAJ thanks the Malaysian Government (Grant number: RG12824-10) and National Defence University of Malaysia for financial support throughout the study period, while JFD thanks the Erasmus programme of the EU. Special thanks to Noriyuki Yamada from Agilent Technologies for the guidance using the ICPMS/MS. The authors thank Dr Corny Brombach for the artwork.

Published on 06 April 2017. Downloaded by University of Aberdeen on 12/04/2017 12:08:14.

Journal of Analytical Atomic Spectrometry Accepted Manuscript

Please do not adjust margins

View Article Online
DOI: 10.1039/C7JA00051K

Please do not adjust margins

Published on 06 April 2017. Downloaded by University of Aberdeen on 12/04/2017 12:08:14.

Journal of Analytical Atomic Spectrometry Accepted Manuscript

Table 3 Calibration data, instrumental LOD and LOQ of fluoride and fluoroacetate using HPLC-ICPMS/MS speciation method.

F compound	Retention time, RT ± SD (min)	Sensitivity (counts L mg^{-1} s^{-1})	Intercept (counts s^{-1})	R^2	LOD (mg L^{-1})	LOQ (mg L^{-1})
Fluoride, F^-	3.66 ± 0.045	24474	3774.3	0.998	0.022	0.085
Fluoroacetic acid, FAA	7.11 ± 0.050	23993	2545.3	0.997	0.11	0.18

Table 4 Limit of detection (LOD) of F analysis using different methods.

Method	Characteristic	Analyte	LOD (concentration)	LOD (in mass)	References
CS-MAS	Molecular absorption	GaF (211.248 nm)	0.26 µg L^{-1}	5.2 pg	31
			1.0 µg L^{-1}	100 pg	32
		SrF (651.187 nm)	36 µg L^{-1}		37
		CaF (606.44 nm)	26 µg L^{-1}	0.26 ng	38
		BaF (495.088 nm)	13 µg L^{-1}	0.13 ng	39
IC	Conductivity	Fluoride	0.03 mg kg^{-1}	0.015 µg	40
			10-50 µg L^{-1}		41
ISE	LaF_3 doped with EuF_2	Fluoride	30 µg L^{-1}		40
			4.55 mg kg^{-1}	1.37 µg	42
ICP-MS	Mass spectrometry	Fluoride: detection as AlF^{2+} on *m/z* 27	0.1 µg L^{-1}		43
HR-ICP-MS	High resolution mass spectrometry	F^+ (*m/z* 19)	5067 µg L^{-1}		28
ETV-ICP-MS	Electrothermal sample introduction to mass spectrometry	F^+ (*m/z* 19)	3200 µg L^{-1}	0.29 µg	44
ICP-AES with tungsten boat furnace vaporiser	Atomic emission spectroscopy	Fluoride ion at analytical line 685.602 nm	71 mg L^{-1}	6.39 µg	45
ICPMS/MS	Triple quadrupole mass spectrometry	BaF^+ (*m/z* 157)	27 µg L^{-1}		34
			43 µg L^{-1}		This work
HPLC-ICPMS/MS	Chromatographic separation with mass spectrometry	BaF^+ (*m/z* 157) for fluoride	22 µg L^{-1}	2.2 ng	This work
		BaF^+ (*m/z* 157) for fluoroacetate	110 µg L^{-1}	11 ng	This work

Table 5 Fluoride and fluoroacetate concentrations and recoveries obtained from HPLC-ICPMS/MS speciation method.

F compounds	F concentration ± SD (mg L^{-1})	Recovery ± SD (%)

This journal is © The Royal Society of Chemistry 20xx

View Article Online
DOI: 10.1039/C7JA00051K

Fluoride, F^-	0.93 ± 0.083	96 ± 11
Fluoroacetate, FAA	0.90 ± 0.087	91 ± 6

Notes and references

1 J. Ekstrand and A. Oliveby, *Acta Odontol. Scand.*, 1999, **57**, 330–333.

2 G. K. Stookey, P. F. DePaola, J. D. B. Featherstone, O. Fejerskov, I. J. Möller, S. Rotberg, K. W. Stephen and J. S. Wefel, *Caries Res.*, 1993, **27**, 337–360.

3 Z. Iheozor-Ejiofor, H. V Worthington, T. Walsh, L. O'Malley, J. E. Clarkson, R. Macey, R. Alam, P. Tugwell, V. Welch and A.-M. Glenny, *Cochrane Database Syst. Rev.*, 2015.

4 J. A. Alvarez, K. M. P. C. Rezende, S. M. S. Marocho, F. B. T. Alves, P. Celiberti and A. L. Ciamponi, *J. Clin. Exp. Dent.*, 2009, **1**, 14–18.

5 A. Queste, M. Lacombe, W. Hellmeier, F. Hillermann, B. Bortulussi, M. Kaup, K. Ott and W. Mathys, *Int. J. Hyg. Environ. Health*, 2001, **203**, 221–224.

6 Y. Li, C. Liang, C. W. Slemenda, R. Ji, S. Sun, J. Cao, C. L. Emsley, F. Ma, Y. Wu, P. Ying, Y. Zhang, S. Gao, W. Zhang, B. P. Katz, S. Niu, S. Cao and C. C. Johnston, *J. Bone Miner. Res.*, 2001, **16**, 932–939.

7 J. K. Fawell and K. Bailey, *Fluoride in drinking-water*, World Health Organization, 2006.

8 J. E. Harwood, *Water Res.*, 1969, **3**, 273–280.

9 van den Hoop, Marc A.G.T, R. F. M. J. Cleven, J. J. van Staden and J. Neele, *Int. Ion Chromatogr. Symp. 1995*, 1996, **739**, 241–248.

10 M. Balcerzak and J. Janiszewska, *Crit. Rev. Anal. Chem.*, 2013, **43**, 138–147.

11 C. M. Butt, U. Berger, R. Bossi and G. T. Tomy, *Sci. Total Environ.*, 2010, 408, 2936–2965.

12 S. Henne, D. E. Shallcross, S. Reimann, P. Xiao, D. Brunner, S. O'Doherty and B. Buchmann, *Environ. Sci. Technol.*, 2012, **46**, 1650–1658.

13 A. Jordan and H. Frank, *Environ. Sci. Technol.*, 1999, **33**, 522–527.

14 M. L. Baron, C. M. Bothroyd, G. I. Rogers, A. Staffa and I. D. Rae, *Phytochemistry*, 1987, **26**, 2293–2295.

15 J. E. Kinnear, M. L. Onus and R. N. Bromilow, *Wildl. Res.*, **15**, 435–450.

16 M. Sanada, T. Miyano, S. Iwadare, J. M. Williamson, B. H. Arison, J. L. Smith, A. W. Douglas, J. M. Liesch and E. Inamine, *J. Antibiot. (Tokyo).*, 1986, **39**, 259–265.

17 S. Taniyasu, K. Kannan, L. W. Y. Yeung, K. Y. Kwok, P. K. S. Lam and N. Yamashita, *Anal. Chim. Acta*, 2008, **619**, 221–230.

18 A. M. Weremiuk, S. Gerstmann and H. Frank, *J. Sep. Sci.*, 2006, **29**, 2251–2255.

19 A. Harsanyi and G. Sandford, *Green Chem.*, 2015, **17**, 2081–2086.

20 M. D. Celiz, J. Tso and D. S. Aga, *Environ. Toxicol. Chem.*, 2009, **28**, 2473–2484.

21 Y. Miyake, N. Yamashita, P. Rostkowski, M. K. So, S. Taniyasu, P. K. S. Lam and K. Kannan, *J. Chromatogr. A*, 2007, **1143**, 98–104.

22 Z. Gong, X. Lu, M. Ma, C. Watt and X. C. Le, *Talanta*, 2002, **58**, 77–96.

23 C. K. Jain and I. Ali, *Water Res.*, 2000, **34**, 4304–4312.

24 P. Politzer, *J. Am. Chem. Soc.*, 1969, **91**, 6235–6237.

25 K. Tsunoda, K. Fujiwara and K. Fuwa, *Anal. Chem.*, 1977, **49**, 2035–2039.

26 K. Kwok, J. E. Carr, G. K. Webster and J. W. Carnahan, *Appl. Spectrosc.*, 2006, **60**, 80–85.

27 J. E. Carr, A. E. Dill, K. Kwok, J. W. Carnahan and G. K. Webster, *Curr. Pharm. Anal.*, 2008, **4**, 206–214.

28 X. Bu, T. Wang and G. Hall, *J. Anal. At. Spectrom.*, 2003, **18**, 1443–1451.

29 G. H. Vickers, D. A. Wilson and G. M. Hieftje, *Anal. Chem.*, 1988, **60**, 1808–1812.

30 S. Morés, G. C. Monteiro, F. D. S. Santos, E. Carasek and B. Welz, *Talanta*, 2011, **85**, 2681–2685.

31 H. Gleisner, J. W. Einax, S. Morés, B. Welz and E. Carasek, *J. Pharm. Biomed. Anal.*, 2011, **54**, 1040–1046.

32 Z. Qin, D. McNee, H. Gleisner, A. Raab, K. Kyeremeh, M. Jaspars, E. Krupp, H. Deng and J. Feldmann, *Anal. Chem.*, 2012, 6213–6219.

33 Z. Qin, A. Raab, E. Krupp, H. Deng and J. Feldmann, *J. Anal. At. Spectrom.*, 2013, **28**, 877–882.

34 N. Yamada, *Feasibility study of fluorine detection by ICP-QQQ*, 2015, vol. 2.

35 M. Resano, P. Marzo, J. Pérez-Arantegui, M. Aramendía, C. Cloquet and F. Vanhaecke, *J. Anal. At. Spectrom.*, 2008, **23**, 1182–1191.

36 E. Bolea-Fernandez, L. Balcaen, M. Resano and F. Vanhaecke, *J. Anal. At. Spectrom.*, 2016, **31**, 303–310.

37 A. R. Borges, L. L. François, B. Welz, E. Carasek and M. G. R. Vale, *J. Anal. At. Spectrom.*, 2014, **29**, 1564.

38 N. Ozbek and S. Akman, *Food Chem.*, 2013, **138**, 650–654.

39 N. Ozbek and S. Akman, *Microchem. J.*, 2014, **117**, 111–115.

40 L. Chan, A. Mehra, S. Saikat and P. Lynch, *Food Res. Int.*, 2013, **51**, 564–570.

41 S. D. Kumar, G. Narayan and S. Hassarajani, *Food Chem.*, 2008, **111**, 784–788.

42 E. Šucman and J. Bednář, *Czech J. Food Sci.*, 2012, **30**, 438–

Published on 06 April 2017. Downloaded by University of Aberdeen on 12/04/2017 12:08:14.

Journal of Analytical Atomic Spectrometry Accepted Manuscript

Please do not adjust margins

View Article Online
DOI: 10.1039/C7JA00051K

441.
43 M. M. Bayón, a Rodríguez Garcia, J. I. García Alonso and a Sanz-Medel, *Analyst*, 1999, **124**, 27–31.
44 Y. Okamoto, *J. Anal. At. Spectrom.*, 2001, **16**, 539–541.
45 Y. Okamoto, N. Yasukawa, T. Fujiwara and E. Iwamoto, *J. Anal. At. Spectrom.*, 2000, **15**, 809–811.

Published on 06 April 2017. Downloaded by University of Aberdeen on 12/04/2017 12:08:14.

Journal of Analytical Atomic Spectrometry Accepted Manuscript

This journal is © The Royal Society of Chemistry 20xx

Please do not adjust margins